Current Optics and Photonics
Vol. 4, No. 6, December 2020, pp. 551-557

ISSN: 2508-7266(Print) / ISSN: 2508-7274(Online)
DOI: https://doi.org/10.3807/COPP.2020.4.6.551

Optical-Loss Measurement of a Silicon-Slab Waveguide

Wildan Panji Tresna[1,2]*, Alexander William Setiawan Putra[1], and Takeo Maruyama[1]

[1]Graduated School of Natural Science and Technology, Kanazawa University, Kanazawa 920-1192, Japan
[2]Research Center for Physics, Indonesian Institute of Sciences, Banten 15314, Indonesia

(Received July 20, 2020 : revised September 7, 2020 : accepted October 6, 2020)

A mirror-in-slab waveguide is fabricated on a slab waveguide by using the refractive-index contrast between two materials, with the reflection performance depending on the slab waveguide's design. In this research, a slab waveguide design consisting of silicon (Si) as the core and SiO_2 as the substrate was designed and developed to determine the coupling, waveguide, and mirror losses. Based on experimental results, coupling loss is dominant and is affected by the design of the slab waveguide. Furthermore, the mirror loss is affected by the design of the mirror, such as the curvature radius and the size of the mirror. TE and TM polarizations of light are used in the measurements. The experimental results show that mirror losses due to reflection by mirrors are 0.011 dB/mirror and 0.007 dB/mirror for TE and TM polarizations respectively. A simulation was performed to confirm whether the size of mirror is sufficient to reflect the input light, and to check the quality of the surfaces of fabricated mirrors.

Keywords : Curved mirror, Propagation loss, Slab waveguide
OCIS codes : (220.2560) Propagating method; (230.4040) Mirrors; (230.7400) Waveguide, slab; (250.5300) Photonics integrated circuits

I. INTRODUCTION

In the world of technology, there are numerous benefits associated with the use of integrated circuits. Some advantages, including efficiency, low energy consumption, and the ability to minimize device size, are due to the use of an optical waveguide as a supporting element. There are two common types of optical waveguides that support the development of many applications, namely the channel waveguide and the slab waveguide [1-4]. Both channel and slab waveguides have a high confinement factor, with the ability to sustain the single-mode condition. The characteristics of a slab waveguide are like those of air. Moreover, cross-section propagation in a slab waveguide occurs without interference loss [5]; on the other hand, in the cross-section propagation of a channel waveguide, loss occurs. Furthermore, due to the confinement factor it is easier to miniaturize a free-space (benchtop) optical system into a slab waveguide.

Some optical components, such as mirrors and lenses, need to be miniaturized from a benchtop optical system to a slab-waveguide optical system. To miniaturize the function of a lens on a slab waveguide, studies have been conducted on various ways to focus the light propagation in a slab waveguide by utilizing a precise trapezoidal design called a *taper*. Moreover, inserting the light from an optical fiber into a slab waveguide is not easy. In some research, spot-size converters have been used in the optical fiber to reduce loss due to coupling [6-13]. In this study, a fiber lens is used to decrease the coupling loss at the input of the slab waveguide. Furthermore, the development of a slab waveguide needs a mirror design, which is constructed based on the difference in refractive index between core and substrate [14-22].

This study examines a silicon-based optical slab waveguide, in terms of design and measurement conditions, built from Si as the core with SiO_2 and air as the substrate and upper layer respectively. Therefore, incident light with a wavelength λ of 1550 nm is confined and guided in the Si core region, with a 45-degree-angle mirror designed and

*Corresponding author: wildanpanji@gmail.com, ORCID 0000-0002-7961-0500
Color versions of one or more of the figures in this paper are available online.

fabricated to reflect the light [23-32]. The propagation loss and mirror loss are also analyzed to determine the performance [33-39].

One purpose of this research is to develop a miniaturized optical technology which is similar to the size of a chip. There are many large-scale benchtop optical systems such as interferometers, beam splitters, and optical encryption systems that need to be miniaturized to chip scale. However, to achieve this purpose some optical components such as mirrors and lenses used in large-scale benchtop optical systems need to be designed on a chip scale.

II. DESIGN ISSUES AND SIMULATION

2.1. Design of the Slab Waveguide

The design of a Si slab waveguide, consisting of a taper and a mirror, is shown in Fig. 1.

In this design the thickness of the slab is 0.21 µm, with an input width of 0.4 µm. These dimensions are designed to carry the single-mode condition of light. In addition, Si and SiO_2 have refractive indices $n_f = 3.4469$ and $n_s = 1.4440$ respectively, at 1550 nm.

2.1.1. Linear taper

A linear taper is adapted to this design, as shown in Fig. 1(a). The function of the taper is to control the divergence angle of the light that is fed into the slab waveguide. The design of the taper is optimized by measuring the *Full Width Half Maximum* (FWHM) of the light after propagation in a *Finite Different Time Domain* (FDTD) simulation. Based on the results, the optimized taper design is obtained when its length L_T and width W_L are 124 µm and 10 µm respectively. This value is the optimal length to get a small diffraction angle of light during propagation in the waveguide. Using this structure, the divergence angle of the input light of the slab waveguide is minimized.

2.1.2. Mirror design

The light is reflected during propagation in the slab waveguide using a mirror. The proposed design with a certain radius of curvature, in accordance with the concave-mirror rule that has a focal point at half of the radius *R*, is shown in Fig. 1(a). The radius *R* (110 µm) and width *S* (24 µm) of the mirror are correlated with the distance between the two mirrors, which is varied to be 50 µm, 100 µm, and 200 µm. The performance of this mirror is measured by its loss. This research proposes to use a curved mirror to reduce the coupling loss due to the mismatch in size between the wavefront of propagated light and the mirror (called *mirror coupling loss*).

2.2. Simulation

FDTD simulations are used to investigate the effect of the tapered design, as shown in Fig. 2. This design sustains the parallel pattern of the light with a small divergence angle. The taper keeps the divergence angle of incident light small. Therefore, the optical power tends to be measured

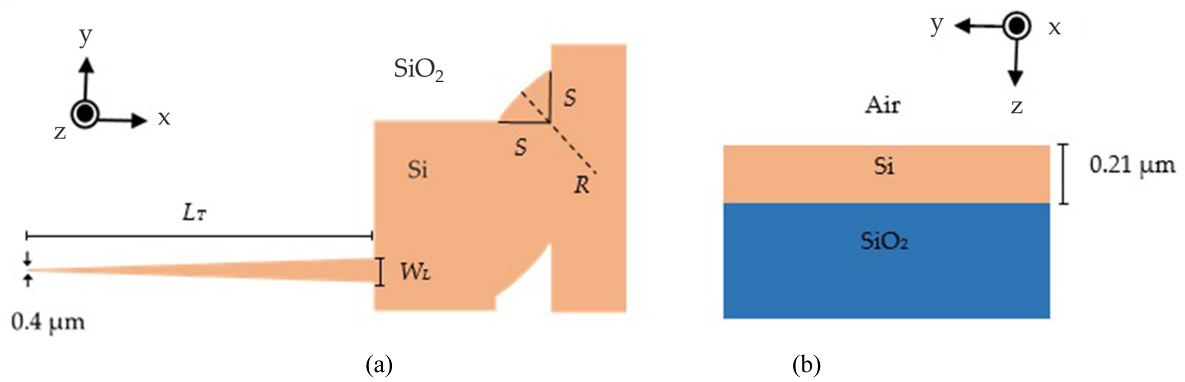

FIG. 1. Design and cross section of the slab waveguide: (a) Design of the slab waveguide in top view, including taper and mirrors. (b) Cross section of the slab waveguide, consisting of SiO_2 and Si as substrate and core, respectively.

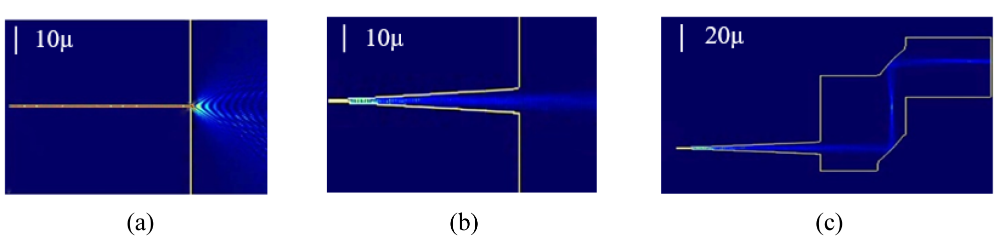

FIG. 2. Simulation results: (a) and (b) for the slab waveguide without and with the tapered design. (c) for showing incident light coming from the tapered design, passing through the slab waveguide, and reflected on the mirrors.

at a long distances.

Figure 2(c) shows that the light propagation is detected at a long distance of 50 μm between mirrors, despite it not being straight propagation. In the simulation, the power analysis is obtained by introducing a power monitor. Furthermore, analysis of the power monitor before and after the mirror positions aids in obtaining the value of the loss due to the scattering that occurs during reflection from a mirror. A curvature radius of 110 μm for the first mirror focuses the light at the midpoint between the first and second mirrors, with a narrower beam at the curvature, as shown in Fig. 2(c). Therefore, the curvature radius of the mirror has to be designed carefully. For clarity, the simulation result for a 4-mirror slab-waveguide system can be seen in Fig. 3.

III. EXPERIMENTAL METHOD

The loss measurements are performed by introducing the light from an optical fiber into the slab waveguide and measuring the output optical power of the waveguide using an optical-power meter, as seen in Fig. 4. A *Polarization-Maintaining Fiber* (PMF) used to preserved the linear polarization during propagation. Furthermore, a lens fiber is used before the slab waveguide to minimize coupling loss, which occurs due to the different sizes of the output and input ports of the fiber and waveguide respectively. A photograph of the fabricated slab waveguide can be seen in Fig. 5.

The rotational wave plate forces the incident light to become polarized as TE or TM. It consists of a half-wave plate (HWP) and a quarter-wave plate (QWP), which are combined to generate a polarization mode, as shown in Fig. 4. A tunable semiconductor laser with a wavelength of 1550 nm and an output optical power of 1 mW is used as the light source.

From the experimental results, the total loss is calculated as the ratio of optical power before (P_{in}) and after (P_{out}) the slab waveguide. This total loss consists of coupling, waveguide, and mirror losses, as seen in Eq. (1):

$$Total\ loss = Coupling\ loss + Waveguide\ loss + Mirror\ loss. \quad (1)$$

The coupling loss occurs at the mounting point between the optical fiber and slab waveguide when inputting the

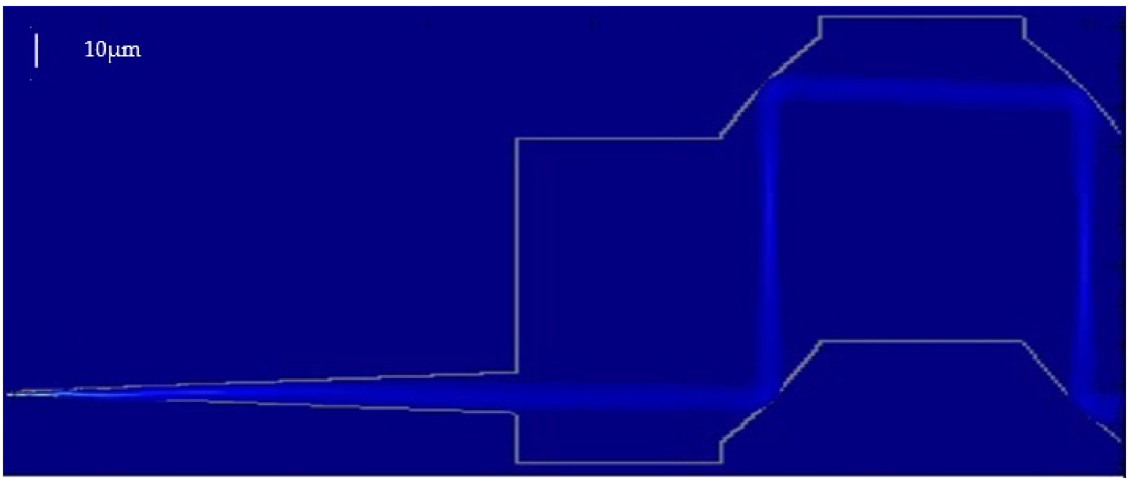

FIG. 3. Simulation of 4 mirrors in a slab waveguide.

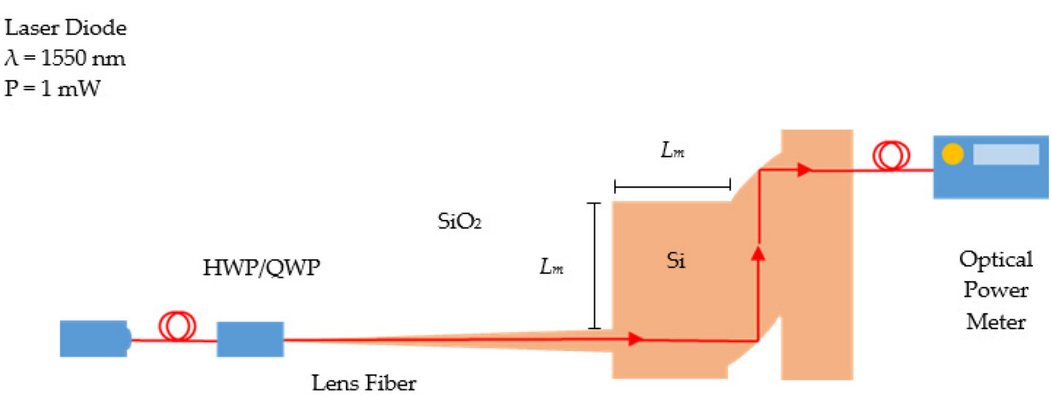

FIG. 4. Experimental setup for the measurement of propagation loss in the slab waveguide.

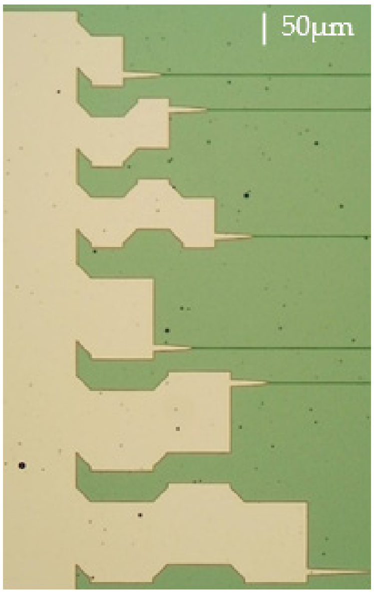

FIG. 5. Photograph of the fabricated Si slab waveguide with mirror structures.

light, and also between the slab waveguide and optical-power meter at the output. To decrease this loss, a fiber lens and wide-core-diameter multimode fiber are used at the input and output of the waveguide respectively. Furthermore, the loss tends to occur due to scattering during propagation and upon reflection from the mirror, which is caused by the surface roughness of the fabricated mirror and the size mismatch between the wavefront of propagated light and mirror in the slab, which in turn depends on the propagation length and mirror design.

IV. RESULTS AND DISCUSSION

4.1. Experimental Results

First, the ratio between the output and input optical powers (the latter being 1 mW) is used to express the total loss. Experiments with three different numbers of mirrors in a slab waveguide for TE and TM polarizations of input light are conducted, with the results shown in Fig. 6.

The propagation loss, which includes waveguide loss α_{wg} and mirror loss α_m, is analyzed from the gradients of trend lines. The other part is the coupling loss, which is loss at zero propagation length. For TE polarization the values of coupling loss are 21.34, 21.27, and 21.17 dB for slab waveguides with 2, 4, and 6 mirrors respectively. Meanwhile, for TM polarization the losses are 19.30, 19.26, and 19.20 dB for slab waveguides with 2, 4, and 6 mirrors respectively. From the gradients of the trend lines in Fig. 6, Fig. 7 is created, to separate the component of total propagation loss that is independent of the number of mirrors (net waveguide loss) from those that depend on the number of mirrors (mirror loss, which includes mirror

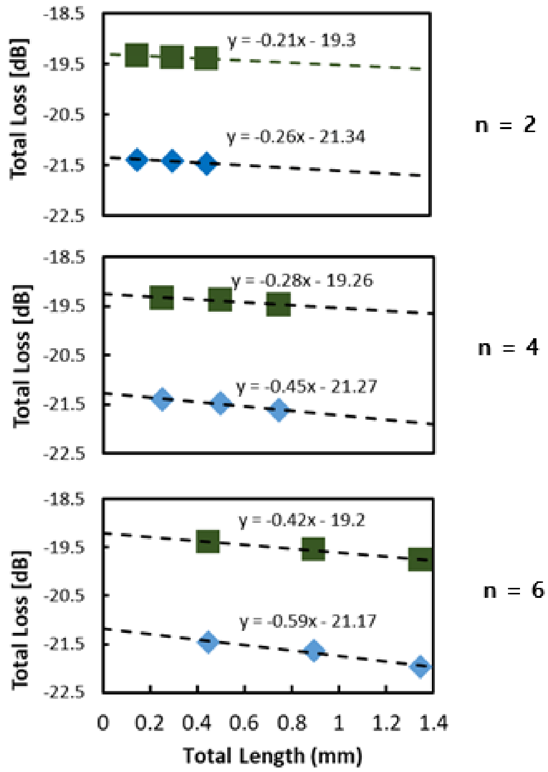

FIG. 6. The dependence of total loss on the length of the slab waveguide. *n* is the number of mirrors.

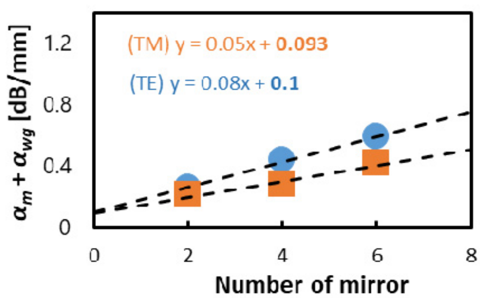

FIG. 7. The dependence of total loss (after subtraction of coupling loss) on the number of mirror.

coupling loss and mirror reflection loss). It is also found that total propagation loss increases with increasing waveguide length, and with the number of mirrors.

Second, α_{wg} and α_m are calculated by analyzing the dependence of the gradients of the trendlines of Fig. 6 on the number of mirrors. The net waveguide losses for TE and TM polarizations, which are 0.10 dB/mm and 0.09 dB/mm respectively, are identified from the linear regression in Fig. 7.

Then the waveguide propagation loss can be calculated using Eq. (2):

$$Waveguide\ loss = Net\ waveguide\ loss \times Waveguide\ length. \quad (2)$$

The mirror loss is equal to the total loss minus the coupling and waveguide propagation losses. After calculating the waveguide loss, the mirror loss α_m is obtained. The linear regression in Fig. 8 needs to be adjusted to obtain a zero value. Then the losses are categorized based on the distance between mirrors L_m.

The total mirror loss increases with increasing distance. Here the highest loss occurs when $n = 6$ and $L_m = 200$ μm. Furthermore, the average mirror loss, which is not affected by the distance, is analyzed in Fig. 9. This is calculated from each value of 2, 4, and 6 mirrors using the linear regression in Fig. 9.

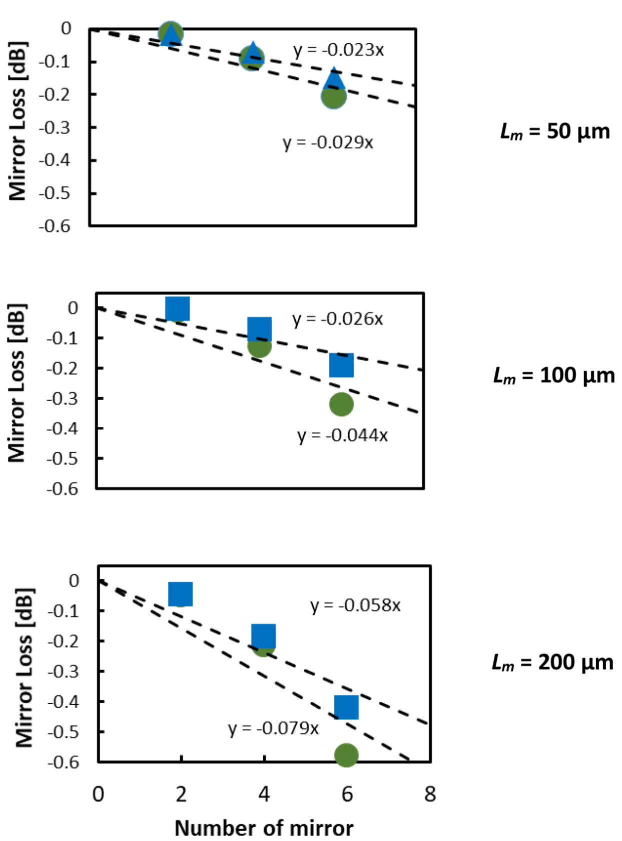

FIG. 8. The dependence of mirror loss on the number of mirrors in the slab waveguide. L is the distance between mirrors.

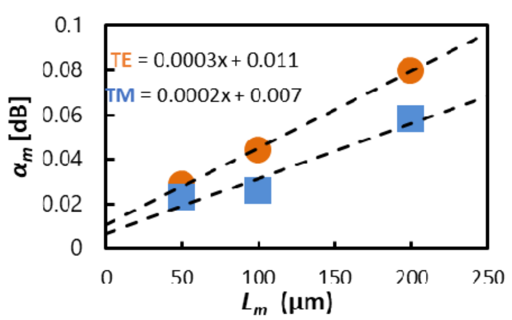

FIG. 9. Calculation of the average mirror loss in the slab waveguide.

The gradients of linear regression in Fig. 9 show the average mirror coupling losses for TE and TM polarization modes, which occurs due to the size mismatch between mirror and wavefront of the propagated light, and the average mirror scattering loss. Based on the experimental results, the average mirror losses due to scattering upon reflection from the mirrors are 0.011 dB/mirror and 0.007 dB/mirror for the TE and TM modes respectively.

4.2. Discussion

According to the experimental data, the mirror scattering losses of the slab waveguide are 0.011 dB/mirror and 0.007 dB/mirror for TE and TM polarizations of light respectively, while the average waveguide losses are 0.1 dB/mm and 0.09 dB/mm. These experimental results are also due to the scattering by the material during the light propagation.

To calculate the mirror loss in the FDTD simulation, two power monitors are set before and after the mirror. By comparing the power before and after the mirror, the loss can be analyzed. The simulation results show the average losses at the mirror are 0.00055 dB and 0.00049 dB for TE and TM polarizations respectively. These values are much smaller than the other losses under consideration that they can be safely neglected. In the simulation an ideal condition is set, without any scattering losses upon reflection from the mirror. While this loss is observed in experiment, due to the mirror's surface roughness and the imperfection in the fabrication of the mirror in the slab waveguide, it cannot be found in the simulation results, because under ideal conditions all of the incoming light is reflected by the 45°-mirror structures of the slab waveguide. The loss in the simulation is only caused by the size mismatch between mirror and wavefront of light. The small values of mirror loss in the simulations show that the design of our mirror and taper structures are sufficient to guide the light properly in the slab waveguide. The tendencies of both simulation and experimental results are similar for both TE and TM polarizations: The mirror loss increases as the distance between mirrors becomes longer, showing that the loss by mirror structures in a slab waveguide is mainly caused by the size mismatch between the propagated light and mirror, not by the scattering upon reflection from the mirror.

V. CONCLUSION

All properties of propagation loss, consisting of coupling, waveguide, and mirror components, in our proposed slab waveguide were investigated. The coupling losses at the input and output ports were the dominant factors, and were reduced by using a lens fiber to conduct the light into the waveguide. In addition, the surface roughness of a fabricated mirror and its fabrication defects also influenced mirror loss: 0.011 dB/mirror and 0.007 dB/mirror for TE and TM polarizations respectively. Conversely, FDTD simulation results showed mirror losses of 0.00055 dB and 0.00047 dB for TE and TM polarizations respectively. The FDTD simulations were used to confirm whether the parameters in the design of the mirror, such as size and curvature radius, were sufficient to reflect all of the light that is guided in the slab waveguide. The small values of mirror losses obtained from the simulation showed that our design was optimized for guiding the light in the slab waveguide with negligible losses due to the size mismatch between mirror and wavefront of the guided light.

ACKNOWLEDGMENT

The first author is grateful for financial support by RISET-Pro, Ministry of Research and Technology / National Research and Innovation Agency of the Republic of Indonesia (Kemenristek/BRIN).

REFERENCES

1. R. N. Noyce, "Large scale integration: what is yet to come?," Science **195**, 1102-1106 (1977).
2. R. Ulrich and R. J. Martin, "Geometrical optics in thin film light guides," Appl. Opt. **10**, 2077-2085 (1971).
3. J. T. Boyd, R. W. Wu, D. E. Zelmon, A. Naumaan, H. A. Timlin, and H. E. Jackson, "Planar and channel optical waveguides utilizing silicon technology," Proc. SPIE **517**, 100-105 (1985).
4. X. Zheng and A. V. Krishnamoorthy, "Si photonics technology for future optical interconnection," in *Proc. Asia Communications and Photonics Conference and Exhibition-ACP* (Shanghai, China, Nov. 2011), pp. 1-11.
5. P. J. Bock, P. Cheben, J. H. Schmid, J. Lapointe, A. Delâge, D.-X. Xu, S. Janz, A. Densmore, and T. J. Hall, "Subwavelength grating crossings for silicon wire waveguides," Opt. Express **18**, 16146-16155 (2010).
6. A. M. Scheggi, R. Falciai, and M. Brenci, "Radiation characteristics of tapered slab waveguides," J. Opt. Soc. Am. **73**, 119-121 (1983).
7. S. Dwari, A. Chakraborty, and S. Sanyal, "Analysis of linear tapered waveguide by two approaches," Prog. Electromagn. Res. **64**, 219-238 (2006).
8. P. Bienstman, S. Aseffa, S. G. Johnson, J. D. Joannopoulos, G. S. Petrich, and L. A. Kolodziejski, "Taper structures for coupling into photonic crystal slab waveguides," J. Opt. Soc. Am. B **20**, 1817-1821 (2003).
9. J. H. Karp, E. J. Tremblay, and J. E. Ford, "Planar micro-optic solar concentrator," Opt. Express **18**, 1122-1133 (2010).
10. H. R. Stuart, "Waveguide lenses with multimode interference for low-loss slab propagation," Opt. Lett. **28**, 2141-3143 (2003).
11. S. Misawa, M. Aoki, S. Fujita, A. Takaura, T. Kihara, K. Yokomori, and H. Funato, "Focusing waveguide mirror with a tapered edge," Appl. Opt. **33**, 3365-3370 (1994).
12. R. Rogozinski, "Planar gradient tapered waveguide in glass," Opto-Electron. Rev. **9**, 326-330 (2001).
13. T. Saastamoinen, M. Kuittinen, P. Vahimaa, and J. Turunen, "Focusing of partially coherent light into planar waveguides," Opt. Express **12**, 4511-4522 (2004).
14. S. Wiechmann, H. J. Heider, and J. Műller, "Analysis and design of integrated optical mirrors in planar waveguide technology," J. Lightwave Technol. **21**, 1584 (2003).
15. M. Hammer, A. Hildebrandt, and J. Förstner, "Full resonant transmission of semiguided planar waves through slab waveguide step at oblique incidence," J. Lightwave Technol. **34**, 997-1005 (2016).
16. M. Hammer, A. Hildebrandt, and J. Förstner, "How planar optical waves can be made to climb dielectric steps," Opt. Lett. **40**, 3711-3714 (2015).
17. C. Son, B. Kim, J. Shin, and N. Dagli, "Very compact metal slab waveguide reflectors as integrated high reflectivity mirrors on high index contrast waveguides," J. Lightwave Technol. **29**, 2999-3003 (2011).
18. S. T. Lau, T. Shiraishi, P. R. McIsaac, A. Behfar-Rad, and J. M. Ballantyne, "Reflection and transmission of a dielectric waveguide mirror," J. Lightwave Technol. **10**, 634-643 (1992).
19. K. Watanabe, J. Schrauwen, A. Leinse, D. V. Thourhout, R. Heideman, and R. Baets, "Total reflection mirror fabricated on silica waveguides with focused ion beam," Electron. Lett. **45**, 883-884 (2009).
20. J.-H. Kim and R. T. Chen, "A collimation mirror in polymeric planar waveguide formed by reactive ion etching," IEEE Photonic Tech. Lett. **15**, 422-424 (2003).
21. K. Tsukamoto, A. Sugama, Y. Wakino, T. Miyashita, and M. Kato, "Simple micro-lens with polymer-filled trench in slab waveguide," Fujitsu Sci. Tech. J. **38**, 54-63 (2002).
22. L. Faustini, C. Coriasso, A. Stano, C. Cacciatore, and D. Campi, "Loss analysis and interference effect in semiconductor integrated waveguide turning mirrors," IEEE Photonic Tech. Lett. **8**, 1355-1357 (1996).
23. F. J. Schműckle and R. Pregla, "The method of lines for the analysis of lossy planar waveguides," IEEE Trans. Microw. Theory Tech. **38**, 1473-1479 (1990).
24. M. R. Ramadas, E. Garmire, A. K. Ghatak, K. Thyagarajan, and M. R. Shenoy, "Analysis of absorbing and leaky planar waveguides: a novel method," Opt. Lett. **14**, 376-378 (1989).
25. M. Kawachi, "Silica waveguides on silicon and their application to integrated-optic components," Opt. Quant. Electron. **22**, 391-416 (1990).
26. J. F. Bauterst, M. J. R. Heck, D. D. John, J. S. Barton, C. M. Bruinink, A. Leinse, R. G. Heideman, D. J. Blumenthal, and J. E. Bowers, "Planar waveguides with less than 0.1 dB/m propagation loss fabricated with wafer bonding," Opt. Express **19**, 24090-24101 (2011).
27. J. J. Ackert, K. J. Murray, P. E. Jessop, and A. P. Knights, "Photodetector for 1550 nm formed in silicon-on-insulator slab waveguide," Electron. Lett. **48**, 1148-1150 (2012).
28. B. D. Jennings, D. McCloskey, J. J. Gough, T. Hoang, N. Abadía, C. Zhong, E. Karademir, A. L. Bradley, and J. F. Donegan, "Characterisation of multi-mode propagation in silicon nitride slab waveguide," J. Opt. **19**, 015604 (2017).
29. R. Ramponi, R. Osellame, and M. Marangoni, "Two straightforward methods for the measurement of optical losses in planar waveguides," Rev. Sci. Instrum. **73**, 1117-1120 (2002).

30. Y. Okamura, S. Yoshinaka, and S. Yamamoto, “Measuring mode propagation losses of integrated optical waveguides: a simple method,” Appl. Opt. **22**, 3892-3894 (1983).
31. T. Feuchter and C. Thirstrup, “High precision planar waveguide propagation loss measurement technique using a Fabry-Perot cavity,” IEEE Photonic Tech. Lett. **6**, 1244-1247 (1994).
32. A. Boudrioua and J. C. Loulergue, “New approach for loss measurements in optical planar waveguides,” Opt. Commun. **137**, 37-40 (1997).
33. Y. Morimoto and T. Ishigure, “Low-loss light coupling with graded-index core polymer optical waveguides via 45-degree mirrors,” Opt. Express **24**, 3550-3561 (2016).
34. Y. Morimoto, R. Kinoshita, A. Takahashi, and T. Ishigure, “45-degree mirrors on graded-index core polymer optical waveguides for low-loss light coupling,” in *Proc. IEEE Photonics Conference* (San Diego, CA, USA, Oct. 2014), pp. 48-49.
35. Y. Z. Tang, W. H. Wang, T. Li, and Y. L. Wang, “Integrated waveguide turning mirror in silicon-on-insulator,” IEEE Photonic Tech. Lett. **14**, 68-70 (2002).
36. W. A. Challener, C. Mihalcea, C. Peng, and K. Pelhos, “Miniature planar solid immersion with focused spot less than a quarter wavelength,” Opt. Express **13**, 7189-7197 (2005).
37. R. Orobtchouk, S. Laval, D. Pascal, and A. Koster, “Analysis of integrated optical waveguide mirrors,” J. Lightwave Technol. **15**, 815-820 (1997).
38. J. Zhang, Y. Zhang, J. Xu, S. B. Lin, and C. X. Liu, “Planar and ridge waveguides formed by proton implantation and femtosecond laser ablation in fused silica,” Vacuum **172**, 109093 (2020).
39. J. Zhang, W. T. Guo, C. Y. Tang, S. Yan, W. N. Li, and C. X. Liu “Planar and ridge waveguides in Yb3+-doped silicate glasses fabricated by proton implantation and precise diamond blade dicing,” Opt. Commun. **453**, 12434 (2019).